Hairline Fracture Detection using MRF and Gibbs Sampling

A. S. Chowdhury[1], A. Bhattacharya[2], S. M. Bhandarkar[1], G. S. Datta[2], J. C. Yu[3], R. Figueroa[4]

(*ananda@cs.uga.edu*, *archanb@stat.uga.edu*, *suchi@cs.uga.edu*, *gauri@stat.uga.edu*, *jyu@mcg.edu*, *rfiguero@mcg.edu*)

[1]*Department of Computer Science*
The University of Georgia
Athens, GA 30602 – 7404, USA.

[2]*Department of Statistics*
The University of Georgia
Athens, GA 30602 – 1952, USA.

[3]*Department of Plastic Surgery*
Medical College of Georgia
Augusta, GA 30912 – 4080, USA.

[4]*Department of Radiology*
Medical College of Georgia
Augusta, GA 30912 – 4080, USA.

Abstract

Detection of hairline fractures, representing points or areas of discontinuity in the bone, is a clinically challenging task, especially in presence of noise. The above problem is equally appealing from a computer vision or pattern recognition perspective since (a) traditional techniques for detection of corners, denoting points of surface discontinuity, typically fail in such cases and, (b) one needs to implicitly handle unknown local degradation in the image. A novel two-phase scheme for hairline mandibular fracture detection, that is robust to noise, is proposed. In the first phase, the hairline fractures are coarsely localized using statistical correlation and by exploiting the bilateral symmetry of the human mandible. In the second phase, the fractures are precisely identified and highlighted using a Markov Random Field (MRF) modeling approach coupled with Maximum A Posteriori probability (MAP) estimation. Gibbs sampling is used to maximize the posterior probability. Experimental results on Computer Tomography (CT) scans from real patients are presented.

Keywords

Computer Tomography, Gibbs Sampling, Hairline Fractures, MRF, MAP.

1. Motivation

Craniofacial fractures, especially mandibular fractures, are quite common now-a-days with the major causes being gunshot wounds, motor vehicle accidents and sports-related injuries [6]. The frequently encountered craniofacial and mandibular fractures are observed to possess distinct patterns in X-ray or Computer Tomography (CT) images [9]. In some cases, the fractures are observed to be hairline or minor in nature. The term *hairline fracture* or *minor fracture* refers to those situations where the broken bone fragments are not visibly out of alignment. In the presence of noise, the detection and subsequent visualization of hairline fractures is a clinically challenging task. In this paper, we propose a novel scheme for hairline mandibular fracture detection in CT images based on Markov Random Field (MRF) modeling and Gibbs sampling. The hairline fracture detection approach is additionally capable of *target pattern generation*, i.e. our method can predict how a jaw with a hairline fracture would appear if allowed to heal naturally without explicit surgical intervention. This may have potential prognostic significance because surgeons can use this to help deciding if open surgical reduction and fixation is indicated or the fractures can be managed by allowing them to heal spontaneously based on what the spontaneously *healed* mandible will be like. From the perspective of computer vision and pattern recognition research, the problem of detection of hairline or minor fractures in X-ray or CT images is inherently challenging. This is so because conventional techniques for detecting points of surface discontinuity, that are typically based on corner detectors such as the Harris detector [4], do not perform well because of the pronounced intensity inhomogeneity and noise present in X-ray or CT images. Moreover, visual comparison of an X-ray or CT image of a mandible with a hairline fracture with that of an unbroken (intact) mandible; reveals changes in pixel intensity only in the vicinity of the fracture site. This results in the formulation of an image restoration problem with a mathematically *unknown local* degradation. This is in sharp contrast to the more conventional image restoration problem with a mathematically *known global* degradation as outlined by Geman and Geman in their classical paper [2].

The proposed fracture detection scheme takes as input a stack of 2D CT image slices of the human mandible with

IEEE Workshop on Applications of Computer Vision (WACV'07)
0-7695-2794-9/07 $20.00 © 2007 IEEE

a hairline fracture. The proposed scheme is modeled as a two-step approach where, in the first step, the hairline fractures are approximately localized within blocks of pixels by exploiting the (approximate) bilateral symmetry of the human mandible and by using statistical correlation of the pixel intensities as a measure of intensity mismatch. Within each of the above pixel blocks, a Markov Random Field (MRF) modeling approach coupled with Maximum A Posteriori (MAP) estimation, along the lines of Geman and Geman [2], is used to achieve hairline fracture detection via implicit image restoration.

1.1 Previous Work and Our Contributions

Existing published literature on fracture detection includes techniques based on exploitation of anatomical knowledge combined with an unconventional *divide-and-conquer* approach [10]; active contour modeling coupled with shape constraints [5], and texture analysis [13]. Our previous work resulted in a novel semi-automated fracture detection scheme [14]; however it was restricted to the class of well-displaced fractures, i.e., fractures where the broken fragments were visibly displaced relative to each other. The classical MRF-MAP paradigm proposed by Geman and Geman [2] has been used, over the years, in various image processing and computer vision problems [3], [7], [8], including problems in medical imaging [12]. However, to the best of our knowledge, the classical MRF-MAP paradigm has not been previously applied to the problem of fracture detection in medical images (X-ray or CT) in general. The contribution of this paper lies in proposing a novel two-phase hairline fracture detection scheme based on the MRF-MAP paradigm that is robust to the presence of noise. The MRF-MAP paradigm is shown to handle input noise in an explicit and efficient manner. The approximate localization of fractures within pixel blocks in the first phase is shown to result in significant computational savings in the second phase since the MRF modeling and MAP estimation in the second phase, which involves Gibbs sampling, is restricted only to those pixel blocks in the CT image stack which are known to contain potential fractures. The second contribution of the paper, from a theoretical standpoint, arises from the fact that the classical MRF-MAP paradigm is improvised to deal with an *unknown local* degradation of image pixel intensities at the fracture site. This is in contrast to the classical MRF-MAP paradigm which incorporates a *global* and *known* deformation model. The proposed scheme for hairline fracture detection is also designed to implicitly restore the broken mandible at the fracture sites, thus offering the surgeon a prognostic view of the bone healing process.

2. Theoretical Framework

The input to the proposed fracture detection scheme is a stack of 2D CT image slices of the human mandible with a hairline fracture. Each 2D CT image slice is assumed to be parallel to the xy plane whereas the z axis is assumed to be the axial direction along which the CT image slices are acquired. The CT image stack is divided into a number of pixel blocks. The theoretical framework of the proposed two-phase fracture detection and localization scheme is described as follows.

2.1 Fracture Localization

Different anatomical structures within the human body are known to possess different types of symmetry [11]. In the context of our problem, we exploit the (approximate) bilateral symmetry exhibited by the human mandible. In the case of a hairline fracture, since the bone fragments are not visibly out of alignment, the bilateral symmetry is still preserved to a great extent. The general equation of the 3D plane of bilateral symmetry is given by:

$$Ax + By + Cz = D \tag{1}$$

For an axial CT scan of the human mandible we assumed B and C to be approximately equal to zero. and the mandibular cross-section to be approximately centered within each CT image slice of width W. Thus, the approximate plane of bilateral symmetry is reduced to:

$$x = W/2 \tag{2}$$

Now, for every incident pixel g_i with coordinates (x, y, z) in the left half of the mandible with a hairline fracture, a bilaterally symmetric pixel g_i^R with coordinates (x^R, y^R, z^R) can be determined as:

$$x^R = W - x,\ y^R = y,\ z^R = z \tag{3}$$

Two heuristics are exploited to reduce the search space for coarse fracture localization. These heuristics along with their justifications (based on domain knowledge) are given below:

1. Since mandibles are essentially bone structures that typically exhibit higher intensity values in CT images, we seek pairs of pixel blocks with high average intensity. This helps to remove pixel blocks containing artifacts and/or large amounts of soft tissue from further consideration.

2. The mandible is typically larger in size compared to other bones in the CT images of the craniofacial skeleton. Since we are primarily interested in detecting mandibular fractures, we perform a second round of

filtering by applying the connected component labeling algorithm, at the pixel block level rather than at the level of individual pixels, and eliminating components which span only a small number of pixel blocks.

By using the above heuristics, we basically retain only a few (say q) pixel blocks which are deemed to constitute solely the fractured mandible.

Having localized the mandible in the CT image, the next goal is to localize the hairline fracture site within it. This is done by taking a block from the left half of the image, all of whose pixels have x coordinate values: $0 \leq x \leq W/2$, and a corresponding bilaterally symmetric block in the right half of the image, all of whose pixels have x coordinate values $W/2 \geq x \geq W$, and computing the statistical correlation between the two. The correlation coefficient between a typical incident block g, with individual pixels g_i, and its bilaterally symmetric counterpart g^R, with corresponding pixels g_i^R is given by:

$$r(g, g^R) = \frac{1}{(n-1)} \sum_{i=1}^{n} \frac{(g_i - \bar{g})}{(s_g)} \frac{(g_i^R - \bar{g}^R)}{(s_g^R)} \qquad (4)$$

where $\bar{g}$ and $\bar{g}^R$ denote the mean and s_g and s_g^R denote the standard deviation of the pixels within the blocks g and g^R respectively.

Having obtained a value of $r(g, g^R)$ for each pair of pixel blocks (g, g^R), the pixel block pairs are sorted in increasing order of their $r(g, g^R)$ values. Note that the pixel block within the intact (unbroken) half of the mandible will have more pixels with higher intensity values (due to the presence of more bone material) compared to its bilaterally symmetric counterpart which contains the hairline fracture (resulting in some loss of bone material). Thus, the underlying rationale is that pairs of pixel blocks which potentially contain fractures should exhibit a higher intensity mismatch and hence lower correlation values. The user can then choose the best k out of q pixel blocks as sites containing potential hairline fractures. The above technique for coarse fracture localization provides the following two advantages:

1. It achieves computational efficiency by effectively reducing the image size over which the proposed MRF-MAP scheme coupled with Gibbs sampling is to be applied. Thus, instead of applying the proposed MRF-MAP scheme over the entire CT image slice, we do so only over the select k pixel blocks in each CT image slice.

2. It renders the prior shape information in each CT image slice more relevant and more accurate. Instead of determining two quadratic polynomials to describe the inner contour and outer contour of the entire mandible, we now only need to determine the quadratic polynomials that describe the inner and outer contours of the portion of the mandible that appears within each of the selected k pixel blocks.

2.2 Model Description

Suppose we have an image with $m \times n$ pixels. Let $p = m \times n$. Based on the formulation detailed in [2], the pixel intensities in the image can be expressed as

$$g = \Phi(f) + \epsilon \qquad (5)$$

where g, f and ϵ are $p \times 1$ vectors such that g represents the vector of all observed image intensities, f represents the vector of intensities corresponding to the true image and ϵ is zero-mean random Gaussian noise

$$\epsilon \sim N(0, \sigma^2 I_p). \qquad (6)$$

where I_p is the p-th order identity matrix. The function $\Phi(.)$ in equation (5) denotes a known degradation (or perturbation) function. Furthermore, we assume the that true pixel intensity f has a known prior distribution. The conditional autoregressive model (CAR) is one of several typical prior distributions used extensively in the domain of image processing. The CAR model also ensures the Markovian property of the mean of the prior distribution [7]. Therefore,

$$\begin{aligned} p(g|f) &\propto \exp\left\{-\tfrac{1}{2\sigma^2}||g - \Phi(f)||^2\right\} \\ p(f) &\propto \exp\left\{-\tfrac{1}{2\tau^2} f^T (I_p - \gamma N) f\right\} \end{aligned} \qquad (7)$$

where N is the neighborhood matrix given by $N = [n_{i,j}]$ such that

$$n_{i,j} = \begin{cases} 1 & \text{if } \ i \text{ and } j \text{ are neighbors} \\ 0 & \text{otherwise} \end{cases} \qquad (8)$$

The value of γ is chosen appropriately to avoid singularity of the matrix $(I_p - \gamma N)$. Under this formulation, the posterior distribution of f given the observed data g can be shown to be Gibbsian on account of conjugacy under linear degradation.

In the context of hairline fracture detection, we assume that the image of the fractured mandible is a degraded version of some true (perhaps hypothetical) intact mandible. Consequently, the degradation function needs to be formulated in a manner such that if it is applied to the entire true image, i.e., the CT image of the intact mandible, the resulting image should display a hairline fracture at the desired site while retaining the pixel intensity values of the true image everywhere else. Radiologically speaking, a hairline fracture denotes a loss of bone mass and hence a decrease in the Hounsfield unit (image intensity) at the fracture site.

Thus, from equation (5), a simple formulation of the degradation function could be

$$g = Af + \epsilon \tag{9}$$

where A is the degradation matrix of order $p \times p$ consisting of non-zero elements only along the diagonal. For the i-th pixel,

$$g_i = a_i f_i + \epsilon_i \tag{10}$$

where

$$a_i = \begin{cases} \alpha_i & \text{if } i \text{ is a fracture site} \\ 1 & \text{otherwise} \end{cases} \tag{11}$$

for some known $\alpha \in (0, 1)$.

Lemma 1 *For each fixed value of g, the posterior probability $p(f|g)$ is a Gibbs distribution with energy function*

$$U(f|g) = \frac{1}{2\sigma^2}||g - Af||^2 + \frac{1}{2\tau^2} f^T (I_p - \gamma N) f$$

For a detailed proof of the above lemma, the interested reader is referred to [2]. As a special case of the above lemma, we describe the following result. Before we provide the result, let us introduce f_{i-} to denote the neighborhood of f_i.

Lemma 2 *Based on the MRF formulation in equations (6) and (9) – (11), if we assume $E(f_i) = \mu(f_{i-})$ then the posterior distribution of f_i given g_i can be shown to be [1]*

$$f_i|g_i, f_{i-} \sim N\left(\frac{\frac{a_i g_i}{\sigma^2} + \frac{\mu(f_{i-})}{\tau^2}}{\frac{a_i^2}{\sigma^2} + \frac{1}{\tau^2}}, \frac{1}{\frac{a_i^2}{\sigma^2} + \frac{1}{\tau^2}} \right).$$

Proof The posterior distribution of $f_i|g_i, f_{i-}$ can be expressed as

$$\begin{aligned} p(f_i|g_i, f_{i-}) &\propto \exp\left\{ -\tfrac{1}{2\sigma^2}(g_i - a_i f_i)^2 \right. \\ &\qquad \left. -\tfrac{1}{2\tau^2}(f_i - \mu(f_{i-}))^2 \right\} \\ &\propto \exp\left[-\tfrac{1}{2}\left\{ \left(\tfrac{a_i^2}{\sigma^2} + \tfrac{1}{\tau^2} \right) f_i^2 - 2 f_i \left(\tfrac{a_i g_i}{\sigma^2} + \tfrac{\mu(f_{i-})}{\tau^2} \right) \right\} \right] \\ &\propto \exp\left\{ -\frac{\frac{a_i^2}{\sigma^2} + \frac{1}{\tau^2}}{2} \left(f_i - \frac{\frac{a_i g_i}{\sigma^2} + \frac{\mu(f_{i-})}{\tau^2}}{\frac{a_i^2}{\sigma^2} + \frac{1}{\tau^2}} \right)^2 \right\} \end{aligned}$$

□

In the above lemma it should be noted that if $E(f_i|g_i)$ can be seen to be a weighted average of the data and prior mean where the weights are based on the choice of σ and τ. Under this situation, we iteratively draw samples from the posterior distribution using Gibbs sampling. The Gibbs sampling procedure ensures convergence to the MAP estimate of the true image after a sufficient number of iterations [2].

A critical issue in the proposed MRF-MAP formulation described above is determining an appropriate value of α. A necessary prerequisite for determining an appropriate value of α is to acquire some a priori knowledge on the shape of the mandible within the selected pixel blocks in each CT slice. The inner and outer contours of the portion of the mandible within each of the pixel blocks can be essentially approximated by quadratic polynomials with different coefficients. A quadratic polynomial has the general form:

$$y = c_1 x^2 + c_2 x + c_3 \tag{12}$$

For estimating the coefficients c_1, c_2 and c_3 in equation (12), we need to solve three simultaneous equations. This means that one needs to obtain a set of three points $[(x_1, y_1), (x_2, y_2), (x_3, y_3)]$ on the inner contour and outer contour of the portion of the mandible in each of the pixel blocks in each image slice in the CT image stack. The need to obtain so many data points (six data points per pixel block per CT image slice) can be justified as follows:

1. The inner and outer contours of the mandible, appearing in a particular CT image slice, cannot be represented mathematically by a single quadratic polynomial with appropriate translation parameters along the x and y axes. This is because the curvatures of the inner contour and outer contour of the mandible are observed to be quite different.

2. Since the spatial resolution of the image stack is coarser along the z axis (axial direction) compared to the x and y axes, an inner or outer contour of the mandible in two different slices cannot be mathematically approximated by a single quadratic polynomial. This is due to difference in curvatures of an inner or outer contour in two consecutive CT image slices.

In the current implementation, user interaction is required (via computer mouse clicks) to generate all the required data points. Note that a typical set of three points can be located anywhere along the inner or outer contour of the portion of the mandible within the chosen pixel block. Thus, the coefficients of the fitted quadratic polynomial are not particularly sensitive to the choice of the clicked points to the extent that these points lie on the contour (inner or outer) whose equation is being estimated. We are in the process of automating the generation of these input data points. Once the quadratic polynomial for a contour is determined, a set of points satisfying the polynomial (i.e., set of points along the fitted contour) is generated. Typically, most of the points within the set have high intensity values, since they correspond to bone pixels, whereas only a few have low intensity values since they correspond to pixels at a potential fracture site. For potential fracture pixels at a site i, on a given contour the value of α can be assigned as follows:

$$\alpha_i = g_i / \max_i(g_i) \tag{13}$$

where $\max_i(g_i)$ represents the maximum of all the observed pixel intensity values along the contour under consideration.

3. Experimental Results and Analysis

In this section, experimental results of the proposed MRF-MAP scheme on a CT image stack containing a typical hairline fracture are described. Experimental results were restricted to a single case to conserve space. Each 2D CT image slice is of size 512×512 pixels with a grayscale resolution of 8 bits per pixel. The image resolution parameters along the x, y and z axes are 0.38 mm/pixel, 0.38 mm/pixel and 1 mm respectively. The pixel block size (which is a power of 2 in the current implementation) is an input from the user via a graphical user interface (GUI). For the CT image sequences used in the current experiments, the pixel block size was chosen to be 64×64 pixels. This means there were altogether 32 pairs of pixel blocks to be examined. After the two heuristics based on mandible size and bone pixel intensity were applied, only 7 out of 32 pixel blocks were retained. They were arranged in order of increasing value of the correlation coefficient. Finally, 2 out of these 7 pixel blocks were chosen as potential hairline fracture sites.

For the MRF-MAP formulation, we chose a first order neighborhood. In the current implementation, the values of τ and α were both chosen to be 1.0 in order to give the prior and the likelihood an equal weight. The value of γ is chosen to 0.25. The total number of iterations required for possible convergence of the Gibbs sampling procedure (i.e., for the posterior distribution to attain its maximum value) was chosen to be 1000. The execution of each phase in the proposed two-phase scheme was observed to take 1-2 minutes on a 1.73 GHz Intel© Pentium©-M processor. Figure 1 provides a visual depiction and demonstration of the the proposed scheme. The first row represents a typical CT image sequence of a mandible exhibiting a hairline fracture. The CT images clearly show that the two bone fragments involved in the hairline fracture are not visibly out of alignment. This fact helps us to exploit the bilateral symmetry between the two halves of the mandible, despite the presence of the hairline fracture. The second row localizes the fracture within a pixel block using bilateral symmetry and statistical correlation. Both the fractured portion (left half of the mandible) and its symmetric intact counterpart (right half of the mandible) are marked by black boxes. The third row shows the results of precise detection and visualization using the proposed MRF-MAP scheme. Note that whereas the original intensity values at the fracture pixel sites were low (due to bone loss), the reconstructed (restored) intensity values at these sites were high, (which correspond to the bone pixel intensities) on account of MAP estimation via repetitive Gibbs sampling. The pixels showing large intensity difference (between the reconstructed and original) were highlighted (using the color black) for the purpose of visualization.

4. Conclusion and Future Work

In this paper, we presented a novel two-phase scheme for hairline fracture detection in CT image data that is robust to the presence of noise. In the first phase, the hairline fractures are localized within pixel blocks of known size by analyzing all the image slices in the CT image stack by exploiting the (approximate) bilateral symmetry of the human mandible and using the statistical correlation coefficient as a measure of intensity mismatch. In each of the aforementioned pixel blocks, an MRF-MAP based approach is used to achieve hairline fracture detection via implicit image restoration. Since the implicit reconstruction embedded within the proposed MRF-MAP based technique is designed to mimic the natural bone healing process in the absence of any surgical intervention, the proposed scheme has an important prognostic significance as well. In addition to its aforementioned clinical significance, the problem of hairline fracture detection also has certain noteworthy aspects of theoretical interest from the perspective of computer vision and pattern recognition research. This is primarily because we are faced with the challenging task of dealing with an image with a spatially localized degradation resulting from a mathematically unknown degradation function. Thus, we first computed the degradation matrix from the input data (by fitting quadratic polynomial functions to the inner and outer contours) before applying the Gibbs sampling procedure for the MAP estimation.

One future plan is to incorporate a higher degree of automation within the existing scheme. The current scheme for quadratic polynomial approximation of the contours of the mandible calls for user interaction via mouse clicks; which needs to be automated in order to reduce the burden on the user. The MRF-MAP paradigm described in this paper needs to be extended to build a 3D target mandible, in case of hairline fractures. On the theoretical side, the degradation matrix A needs to be modeled as a stochastic entity, rather than a deterministic one by imposing a suitable prior distribution (such as a Beta distribution) on the α values. We also plan to study the impact of generalization of the A matrix from a strictly diagonal matrix to a banded-diagonal matrix to exploit the spatial distribution of the degradation process. Finally, we propose to formulate prior distributions (such as the Inverse-Gamma distribution) for both τ and σ in order to conform to the hierarchical Bayesian paradigm. With this modified formulation, the posterior distribution may no longer remain Gibbsian which would require alternative sampling scheme such as rejection sampling [1] for drawing samples from the posterior distribution.

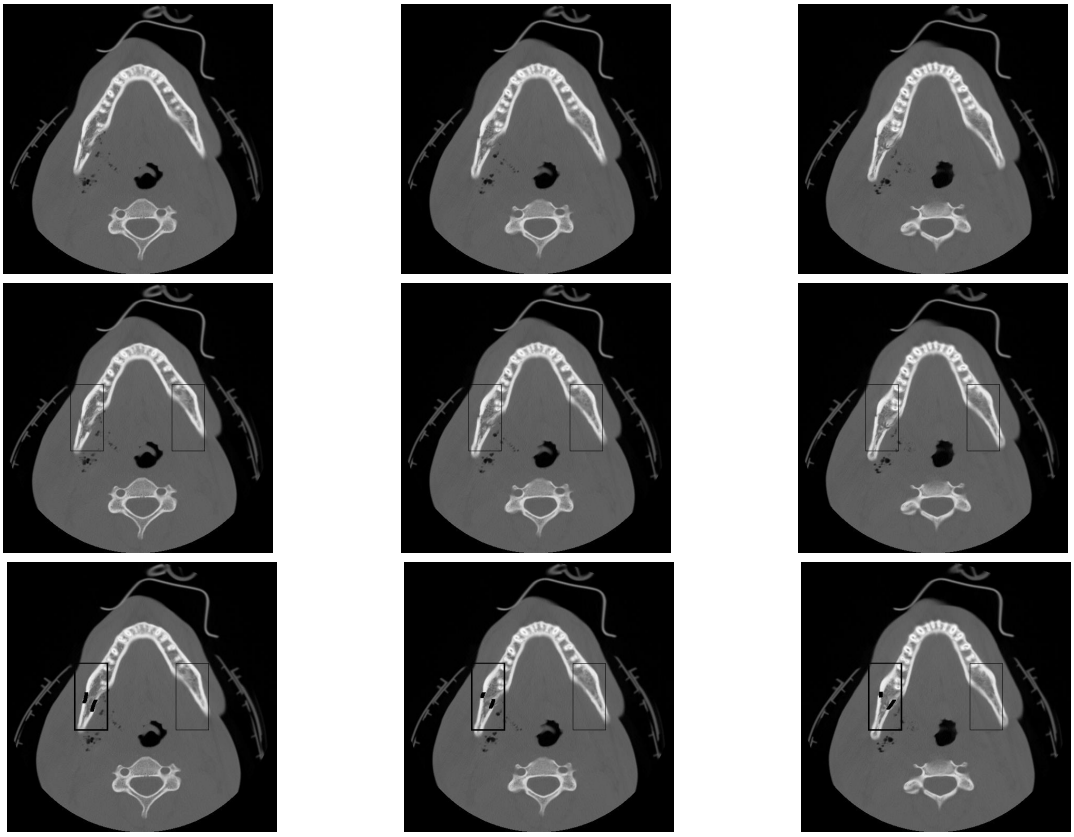

Figure 1: Two-phase fracture hairline detection scheme on a real patient CT image sequence

References

[1] A. Gelman, J.B. Carlin, H.S. Stern and D.B.Rubin, *Bayesian Data Analysis*, Chapman & Hall-CRC, NY, 2004.

[2] S. Geman and D. Geman Stochastic Relaxation, Gibbs Distributions, and the Bayesian Restoration of Images, *IEEE Trans. on Pat. Anal. and Mach. Intel.*, 6(6), pp. 721 - 741, 1984.

[3] I. Hsiao, A. Rangarajan and G. Gindi, Joint MAP Bayesian tomographic reconstruction with a Gamma-mixture prior, *IEEE Trans. on Im. Proc.*, 11(12), pp. 1466-1477, 2002.

[4] C. J. Harris and M. Stephens, A combined corner and edge detector. *Proc. 4th Alvey Vision Conferences*, pp. 147-151, 1988.

[5] Y Jia and Y Jiang, Active Contour Model with Shape Constraints for Bone Fracture Detection, *Proc. of CGIV*, pp. 90-95, 2006.

[6] R.E. King, J.M. Scianna and G.J. Petruzzelli, Mandible Fracture Patterns: a Suburban Trauma Center Experience, *Amer. J. of Otolaryngology*, 25(5), pp. 301-307, 2004.

[7] R. Molina, On the Hierarchical Bayesian Approach to Image Restoration: Applications to Astronomical Images, *IEEE Trans. on Pat. Anal. and Mach. Intel.*, 16(11), pp. 1122-1128, 1994.

[8] R. Molina, A.K. Katsggelos, J. Mateos, A. Hermoso and C.A. Segall, Restoration of severely blurred high range images using stochastic and deterministic relaxation algorithms in compound Gauss-Markov random fields, *Pattern Recognition*, 33, pp. 555 - 571, 2000.

[9] B.O. Ogundare, A. Bonnick and N. Bayley, Pattern of Mandibular Fractures in an Urban Major Trauma Center, *J. of Oral and Maxillofacial Surgery*, 61(6), pp. 713-718, 2003.

[10] T. Ozanian and R. Phillips, Image Analysis for Computer-Assisted Surgery of Hip Fractures, *Med. Im. Anal.*, 4(2),pp. 137 - 159, 2000.

[11] S. Prima, S. Ourselin, and N. Ayache, Computation of the Mid-Sagittal Plane in 3D Brain Images, *IEEE Trans. on Med. Imaging*, 21(2), pp. 122-138, 2002.

[12] C. Popa and R. Zdunek, Penalized Least-Squares Image Reconstruction For Borehole Tomography, *Proc. of Algorithmy*, pp. 260-269, 2005.

[13] D. W. H. Yap, Y. Chen, W. K. Leow, T. S. Howe, and M. A. Png, Detecting Femur Fractures by Texture Analysis of Trabeculae. *Proc. of ICPR*, pp. 730-733, 2004.

[14] A.S. Chowdhury, S.M. Bhandarkar, G. Datta and J.C. Yu, Automated Detection of Stable Fracture Points In Computed Tomography Image Sequences, *Proc. of ISBI*, pp. 1320 - 1323, 2006.